PNAS PLUS

Impact of membrane lipid composition on the structure and stability of the transmembrane domain of amyloid precursor protein

Laura Dominguez[a,b], Leigh Foster[a], John E. Straub[a,1], and D. Thirumalai[c]

[a]Department of Chemistry, Boston University, Boston, MA 02215; [b]Department of Physical Chemistry, School of Chemistry, National Autonomous University of Mexico, Mexico City 04510, Mexico; and [c]Department of Chemistry, University of Texas at Austin, Austin, TX 78712

Edited by Michael L. Klein, Temple University, Philadelphia, PA, and approved July 6, 2016 (received for review April 22, 2016)

Cleavage of the amyloid precursor protein (APP) by γ-secretase is a crucial first step in the evolution of Alzheimer's disease. To discover the cleavage mechanism, it is urgent to predict the structures of APP monomers and dimers in varying membrane environments. We determined the structures of the $C99_{23-55}$ monomer and homodimer as a function of membrane lipid composition using a multiscale simulation approach that blends atomistic and coarse-grained models. We demonstrate that the $C99_{23-55}$ homodimer structures form a heterogeneous ensemble with multiple conformational states, each stabilized by characteristic interpeptide interactions. The relative probabilities of each conformational state are sensitive to the membrane environment, leading to substantial variation in homodimer peptide structure as a function of membrane lipid composition or the presence of an anionic lipid environment. In contrast, the helicity of the transmembrane domain of monomeric $C99_{1-55}$ is relatively insensitive to the membrane lipid composition, in agreement with experimental observations. The dimer structures of human EphA2 receptor depend on the lipid environment, which we show is linked to the location of the structural motifs in the dimer interface, thereby establishing that both sequence and membrane composition modulate the complete energy landscape of membrane-bound proteins. As a by-product of our work, we explain the discrepancy in structures predicted for C99 congener homodimers in membrane and micelle environments. Our study provides insight into the observed dependence of C99 protein cleavage by γ-secretase, critical to the formation of amyloid-β protein, on membrane thickness and lipid composition.

amyloid precursor protein | membrane composition | APP dimer | Aβ peptide | Alzheimer's disease

Understanding the structural and thermodynamic properties of transmembrane (TM) helical dimers is of fundamental importance to molecular biology. It is known that the association of "bitopic" proteins, having single pass TM helical domains, is essential to immunoreceptors and protein kinases that play critical roles in cellular function. Computational and experimental studies have provided insight into the role of sequence-specific interactions stabilizing helix dimerization (1, 2). Examples include the heptad repeat motif responsible for the stability of coiled-coils in GCN4 phospholamban (3) and the M2 proton channel (4), the role of the GxxxG motif in stabilizing TM helix–helix association in systems including the glycophorin A (GpA) homodimer (5, 6), found in the human erythrocyte membrane, and GxxxG and heptad repeat motifs, which play a role in stabilizing homodimers of APP-C99 (C99), the 99-aa C-terminal fragment of the amyloid precursor protein (APP) (7, 8).

The amyloid β (Aβ) peptide aggregation pathway, known to be crucial to the evolution of Alzheimer's disease (AD), begins with the cleavage of C99 by γ-secretase leading to the formation of a number of isoforms of Aβ. The formation of homodimers of C99 has been proposed to be critical to the mechanism by which C99 is cleaved by γ-secretase, a process that is known to depend on a number of factors including peptide sequence (9–13) and lipid composition of the membrane environment (14, 15). However, recent studies have questioned the role (16) and importance (17, 18) of homodimerization in the processing of full-length C99 by γ-secretase. Regardless of whether C99 homodimer is a natural substrate for γ-secretase, its ready formation both in vitro and in vivo raises the question, what is the functional role of the dimer? Additional knowledge of the structure and stability of the C99 homodimer is therefore essential to our fundamental understanding of principles governing TM helix homodimerization and the molecular basis of AD.

The first simulation of an equilibrium structural ensemble of the homodimer of the TM helical region of C99, $C99_{23-55}$, was performed using replica-exchange molecular dynamics (REMD) simulation and an implicit membrane model (8). We found that the structure of the WT homodimer to be a λ-like right-handed coiled-coil structure stabilized by interpeptide C_α hydrogen bonds, mediated by interactions between GxxxG motifs. The results indicated that the GxxxG repeat region was significantly less helical than the C-terminal portion of the TM helix. We observed that, of the three contiguous GxxxG motifs in the WT peptides, residues Gly_{33} and Gly_{38} are most essential in stabilizing the WT dimer through the formation of C_α hydrogen bonds. The predicted structural ensemble was in good agreement with the proposed solid-state NMR structure (7), while providing more quantitative insights into the structural ensemble of the dimer in a fluid membrane environment.

Contemporaneously, using REMD simulations of $C99_{1-55}$ monomer in an implicit membrane model, we predicted that the TM helix has two helical segments separated by a "hinge" at

Significance

Aggregation of proteins of known sequence is linked to a variety of neurodegenerative disorders. Familial mutations in the amyloid precursor protein (APP), from which the amyloid β (Aβ) protein is excised, are associated with early onset of Alzheimer's disease. The structures of APP-C99 dimers and the associated stability as well as the monomer–dimer equilibrium are critically influenced by membrane composition. Using a multiscale modeling approach, we have investigated the influence of varying lipid composition on the structure of homodimers of an APP-C99 congener peptide. Besides resolving contradicting experimental results, we demonstrate that membrane lipid composition dramatically influences the relative populations of competing homodimer structures in a way that is linked to the recognition and processing of APP-C99 by γ-secretase.

Author contributions: J.E.S. and D.T. designed research; L.D., L.F., and J.E.S. performed research; L.D., L.F., J.E.S., and D.T. analyzed data; and L.D., L.F., J.E.S., and D.T. wrote the paper.

The authors declare no conflict of interest.

This article is a PNAS Direct Submission.

[1]To whom correspondence should be addressed. Email: straub@bu.edu.

This article contains supporting information online at www.pnas.org/lookup/suppl/doi:10.1073/pnas.1606482113/-/DCSupplemental.

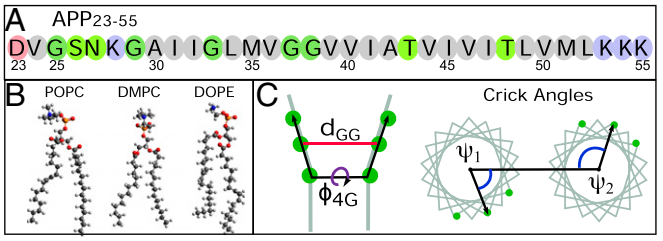

Fig. 1. (*A*) $C99_{23-55}$ sequence. Polar residues are colored in green, negatively charged residues are colored in red, and positively charged residues are colored in blue. (*B*) Structure of lipids used: POPC, DMPC, DOPE. (*C*) Order parameter for structural characterization: d_{GG} is the interhelical distance between G_{33A}–G_{33B}, ϕ_{4G} is the dihedral angle formed by G_{29A}–G_{37A}–G_{37B}–G_{29B}, where *A* and *B* correspond to the two $C99_{23-55}$ monomers. ψ_{Crick} corresponds to the angle between the vector connecting the axis points of the two helices and the vector connecting the interhelical vector formed by residue G_{37}.

Gly_{37}/Gly_{38} (19). This key prediction was validated in a recent study involving H/D exchange experiments on the C99 peptide complemented with molecular dynamics (MD) simulations of the TM region, $C99_{28-55}$, in a 1-palmitoyl-2-oleoyl-*sn*-glycero-3-phosphocholine (POPC) bilayer (20), which also provided detailed insights into the stability of the TM helical region of C99. It was found that the portion of the TM helix on the N-terminal side of the Gly_{37}/Gly_{38} hinge was more dynamic and showed enhanced H/D exchange relative to the C-terminal portion of the TM helix (20), a finding in agreement with studies of the C99 monomer in lyso-myristoyl phosphatidylglycerol (LMPG) micelles (21, 22).

Although there is agreement between different experiments and our predictions on well characterized membranes, there is a great deal of controversy regarding the role of lipid composition on APP structures. Two NMR structures of the C99 homodimer congener peptides in a micelle environment have been reported. The proposed structure of GSQ-$C99_{15-55}$ in dodecyl-phosphocholine (DPC) is a *X*-like left-handed dimer stabilized through interactions involving an extended heptad repeat motif in the C-terminal TM helical region. In contrast, the structure of $C99_{28-55}$ homodimer in DPC micelle is a right-handed coiled-coil in agreement with our simulation results of $C99_{15-55}$ homodimer in DPC micelle (23, 24). These studies raise critical questions related to the peptide environment, focusing on how factors such as micelle size and interfacial curvature might influence peptide structures (25, 26).

An NMR study of monomeric $C99_{1-55}$ in membrane environments of variable lipid composition demonstrated that fluctuations in the TM helix can be a strong function of membrane composition (27), suggesting that changes in membrane composition modulate the physical boundaries of the bilayer, including the width and structure of the interface, as well as the chemical nature of the head group region and membrane interior. On the other hand, structures of $C99_{1-99}$ monomer peptide in LMPG micelles and in a series of five zwitterionic bicelle compositions (phosphatidylcholine and sphingomyelin where the acyl chain lengths varied from 14 to 24 carbons) suggest that the helicity of the TM domain of C99 is relatively insensitive to membrane lipid composition (22, 28). These contrasting conclusions for the structures of both the monomers and dimers raise important questions related to the role of environment in modulating C99 monomer structure and C99 homodimer structure and stability.

To resolve the contradicting reports, we have performed detailed simulations of the structure and stability of the monomer and homodimer of the TM domain of $C99_{23-55}$ using a multiscale computational model. Our approach uses atomistic and coarse-grained (CG) representations of the peptide and lipid system self-consistently in a manner that allows for the study of the homodimer structure and its dependence on membrane composition. The multiscale approach we have developed to model TM helical association in lipid bilayers, critical to biomolecular signaling and processing, can provide important insights into the relationship between protein structure and function. By combining the key structural features discovered here, CG simulations when combined with detailed atomic detailed simulations provide a platform for elucidating the energy landscape of membrane peptide systems in general. Remarkably, for the APP dimer quantitatively identical structures are found independent of the membrane composition. However, the extent of heterogeneity of the homodimer ensemble varies and the ground state structure is ultimately selected by the specific membrane environment. Our study provides a detailed picture of the $C99_{23-55}$ structural ensemble, its dependence on membrane composition, and the potential role for changes in structure to influence cleavage of this critical APP by secretases.

Results

Implicit Membrane REMD and CG MD Simulations. The initial conformational distributions were derived from both REMD or CG MD simulations. REMD simulations consisted of 16 replicas spanning temperatures from 300 to 550 K with 10 ns of simulation for each replica (160-ns total simulation time) for each system. We simulated the $C99_{23-55}$ homodimer systems in four different generalized Born model with a simple switching (GBSW) implicit membrane widths: 27, 30, 32, and 35 Å, respectively. Starting configurations sampled a variety of dimer interfaces, with the peptides initially placed 25 Å apart. CG simulations were performed using 60 replicas with 1.5 μs of dynamics for the $C99_{23-55}$ homodimer in 1,2-dimyristoyl-*sn*-glycero-3-phosphocholine (DMPC), POPC, and 50:50 POPC/1,2-dioleoyl-*sn*-glycero-3-phosphoethanolamine (DOPE) bilayers. The two monomers were initially placed at a separation of 50 Å and allowed to associate. As a consequence of the large initial separation, there are no biases in the association of the monomers.

$C99_{23-55}$ Homodimer Populates Multiple Conformational States. Important order parameters used to characterize the homodimer ensemble include the dihedral angle formed by G_{29}–G_{37}–G_{37}–G_{29} (ϕ_{4G}) (Fig. 1), which differentiates right-handed (negative values) and left-handed (positive values) coiled-coil geometries, and d_{GG} distance, where close distances indicate interpeptide contacts in the GxxxG repeat region. Structural ensembles were also projected onto the space of Crick angles, ψ_{Crick}, where ψ_{Crick} of each peptide is defined as the dihedral angle formed by the center of the G_{29} residue, helix vector, and interhelix vector formed by residues G_{37} (Fig. 1). Simulations of the homodimer were analyzed using a projection of the simulated structural ensemble onto the ϕ_{4G} angle and the d_{GG} distance between the

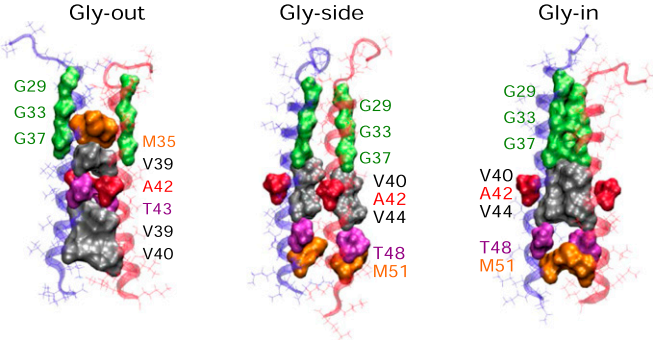

Fig. 2. The different $C99_{23-55}$ dimer interfaces: (*Left*) A $C99_{23-55}$ Gly-out conformation with a right-handed crossing angle between the helices and GxxxG facing the outside of the interface. (*Center*) A $C99_{23-55}$ Gly-side conformation with a right-handed crossing angle between the helices, showing one monomer GxxxG motif facing the interface between the helices and the second monomer GxxxG motif facing the outside of the interface. (*Right*) A $C99_{23-55}$ Gly-in conformation with right-handed crossing angle between the helices and both monomer GxxxG motifs facing the inside of the interface between the monomers.

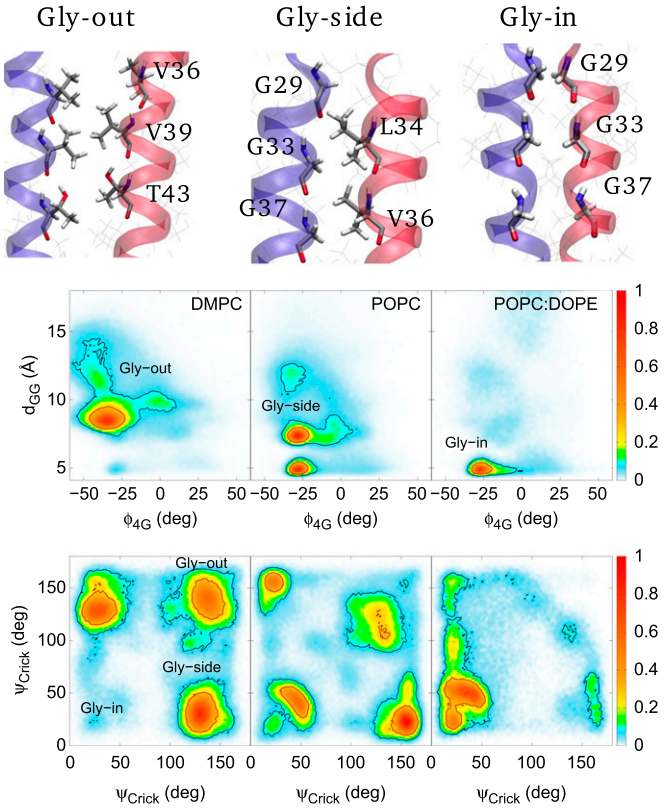

Fig. 3. (*Top*) Key residues located at the interface of $C99_{23-55}$ Gly-out, Gly-side, and Gly-in conformations. (*Bottom*) Conformational distributions of $C99_{23-55}$ dimers derived from CG MD simulations. Although the overall conformational ensemble is dominated by right-handed coiled-coil conformations for each bilayer, the lipid composition is observed to modulate the relative stability of competing states in the homodimer structural ensemble. The colored scale on the *Right* defines the relative populations.

homodimers in bilayers of varying lipid composition as well as the Crick angles, ψ_{Crick} (Fig. 3 and Fig. S1).

We identify three states (Figs. 2 and 3) that characterize the homodimer ensemble, where conformations within each state are uniquely identified in terms of one of three different packing interfaces. (*i*) The most populated state (Gly-in) is stabilized by Gly–Gly interactions in which the residues of the ϕ_{4G} repeat face the inside of the homodimer structure with d_{GG} distances of 5 Å and ϕ_{4G} angles of less than −25°. (*ii*) The next most populated (Gly-side) state is characterized by stabilizing interpeptide interactions involving the hydrophobic residues Leu34 and Met35 that interact to form a zipper-like structure (with glycines facing the side of the homodimer interface). (*iii*) In the least populated (Gly-out) state, glycine repeats face the outside of the homodimer interface leading to stabilization of the homodimer by hydrophobic interpeptide interactions (residues A42, T43, V39, and V40) with a d_{GG} distance of 12 Å.

Figs. 3 and 4 and Fig. S1 display the probability distributions for the ϕ_{4G} angle and d_{GG} distance for the $C99_{23-55}$ homodimer in four different CG and implicit membrane systems, respectively. Although right-handed homodimers are dominant in all membrane compositions, there are notable changes in the relative probability of the three conformational states that compose the homodimer's conformational ensemble. In particular, in moving from the shortest to longest lipid alkyl chains in saturated DMPC, monounsaturated POPC, and finally to the mixture of POPC and diunsaturated DOPE, there is a dramatic shift in populations of the three homodimer substates. The dominate states in each bilayer vary dramatically from DMPC (32% Gly-out) to POPC (18.0% Gly-in and 16.5% Gly-side) to POPC:DOPE (30% Gly-in). The extent of shift is similar in the implicit membrane systems as the GBSW membrane width is increased (Fig. S2) and for the CG models with fully saturated lipids varying only the length of the alkyl chain (Fig. S1).

Lipid Composition Modulates Competing $C99_{23-55}$ Homodimer States. Overall, the particular homodimer structure, and the intrinsic disorder in the conformational ensemble, is a strong function of membrane composition. The shift in state populations can be understood in terms of the lipid and solvent density profiles, as well as the lateral pressure profiles, for the three bilayers (Fig. 5). In the thinnest membrane system, DMPC (CG)/27 Å (GBSW), the homodimer has the broadest distribution of ϕ_{4G} angle, and the most substantial populations in the Gly-out substate. As the lipid composition is varied and the membrane width increases, there is a transition to increasingly sharply defined values of ϕ_{4G} angle and enhanced population of the Gly-in substate. In the thickest membrane, POPC/DOPE, there is a relative stabilization of the Gly-in state that is consistent with the earliest predictions of the $C99_{23-55}$ homodimer structure (8).

As membrane lipid composition is varied from shorter-chained DMPC to longer-chained POPC:DOPE in the all-atom models, and from smaller to wider membranes in the implicit models, a concomitant decrease in the average tilt angle is observed such that the average kink angle is relatively constant (Fig. S2). This suggests that the magnitude of fluctuations in the TM helix about the GG-hinge region, which may play an important role in C99 processing, is an intrinsic characteristic of the TM domain sequence.

All-Atom MD Simulations. To develop a detailed atomistic description of the protein–protein interactions in the most probable CG homodimeric structures, we performed all-atom MD simulations using the CHARMM force field in a variety of lipid membranes and analyzed the resulting structural distributions. The all-atom simulations were used to evaluate the helicity of $C99_{23-55}$ monomer and dimers in varying membrane lipid compositions (Fig. 6), variations in the solvent-accessible surface area (SASA), and the calculation of pressure–volume (pV) work contributions to dimerization (Fig. 5 and Fig. S3 and associated discussion).

Helicity of TM helix is relatively insensitive to homodimer formation. It appears that fluctuations in the monomeric peptide, particularly near the proposed "kink" region of the TM helix, is associated with slightly reduced helicity in the monomer. In the dimeric conformations, this kink is stabilized by the dimer interactions further reducing the average helicity of $C99_{23-55}$ in the dimeric

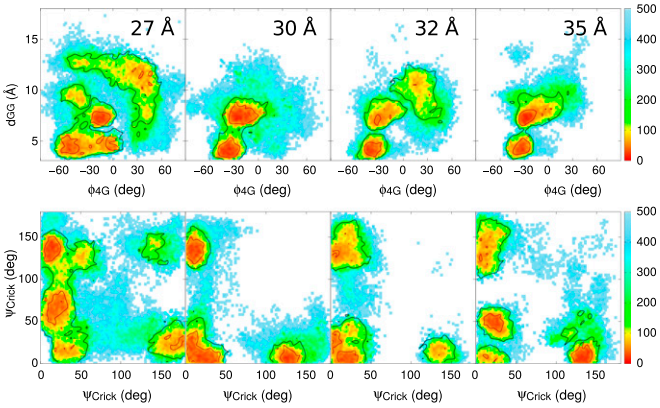

Fig. 4. Conformational distributions derived from REMD simulations of all-atom peptide in GBSW implicit solvent. The simulations favor right-handed structures at lower d_{GG} values, although structures with larger d_{GG} values also sample left-handed structures. The relative sampling of each state shifts as the membrane width increases, with the 32-Å membrane homodimer structural ensemble strongly dominated by the Gly-in state. The colored scale on the *Right* defines the relative free energy calculated (in kilocalories per mole).

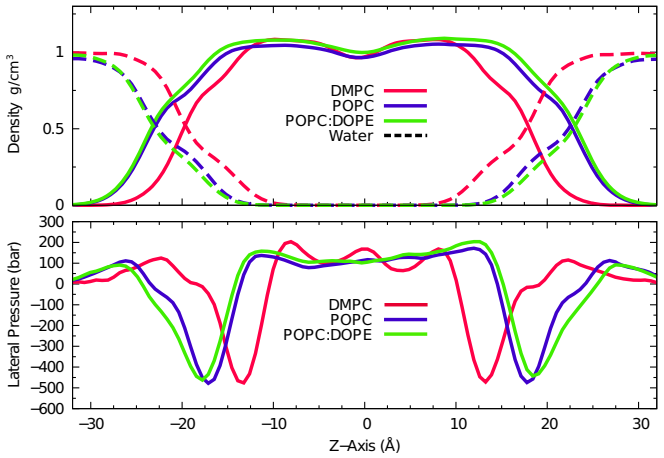

Fig. 5. Lipid (solid lines) and water (dashed lines) density profiles (*Top*) derived from CG MD simulations in DMPC, POPC, and POPC:DOPE bilayers. Lateral pressure profiles (*Bottom*) as a function of lipid composition.

structures. The differences observed are minor and consistent with the view that TM domain helicity is only weakly impacted by dimerization.

Enhanced hydrophobic surface stabilizes Gly-out homodimer in thin membrane and bilayer environments. Our results (Fig. S2) suggest that smaller membrane widths favor larger tilt angles of $C99_{23-55}$ monomers imposing restraints on the formation of favorable GxxxG interactions between $C99_{23-55}$ TM helices. An important difference between the observed Gly-in and Gly-out conformations are the lipophilic and hydrophilic properties of the molecular surface as a response to a hydrophobic mismatch. Gly-out conformations present a larger overall exposed surface area and larger fraction of hydrophobic surface area than Gly-in conformations. It is likely that deeper water penetration (Fig. 5, *Top*) in the thinner DMPC bilayer and micelle environments stabilizes the Gly-out homodimer structure that presents more absolute hydrophilic surface area than the Gly-in structure.

The calculated SASA values of the $C99_{23-55}$ TM helix (from A30 to L52) derived from all-atom simulations of $C99_{23-55}$ homodimers in a POPC membrane are ~ 2,800 Å^2 (hydrophobic) and ~ 325 Å^2 (hydrophilic) for Gly-in and ~ 3,100 Å^2 (hydrophobic) and ~ 430 Å^2 (hydrophilic) for Gly-out state. The Gly-out structures show a larger hydrophobic SASA due to higher exposure of bulky hydrophobic amino acids located at the TM-N homodimer interface and exposure of the outward-facing Gly interface created by the GxxxG motif. On the other hand, the Gly-in conformation presents a more elongated structure with smaller volume as a function of the Z coordinate and reduced SASA (smaller hydrophilic and hydrophobic surface area).

pV work favors formation of more compact Gly-in homodimer in POPC bilayer. A key characteristic of the environment of membrane proteins is the lateral pressure profile. The heterogeneity of the surrounding lipid or surfactant environment, with contributions from water, polar, or charged head groups, and lipophilic acyl chains, leads to a nonuniform pressure profile as a function of depth in the bilayer. The characteristics of the pressure profile are known to depend on lipid composition within a given geometry, such as a bilayer, as well as the geometry of the lipid environment, including the curvature at a bilayer, micelle, or vesicle interface. Cantor has explored the influence of lateral pressure profiles on membrane protein structure and function (30–32), including the conductance of ion channels (33) and protein association (34). We analyzed the pressure field surrounding a protein complex encapsulated in a POPC bilayer and assessed the impact of the spatially-dependent pV work on the relative stability of $C99_{23-55}$ monomer and homodimer conformations.

The pV work contribution to the free energy of dimerization can be written as follows:

$$w_{pV} = \int_{-\infty}^{\infty} p(z)\Delta A(z)dz, \quad [1]$$

where $\Delta A = A_D(z) - A_M(z)$ is the relative difference in area of the dimer and two monomers and $V_D = \int_{-\infty}^{\infty} A_D(z)dz$ and $V_M = \int_{-\infty}^{\infty} A_M(z)dz$ are the volumes of the dimer and monomers, respectively. With $p(z) > 0$ and independent of z, the w_{pV} would be as follows:

$$w_{pV} = p(V_D - V_M), \quad [2]$$

and $V_D < V_M$ would result in $w_{pV} < 0$ lowering the relative free energy of the dimer compared with the separated monomers and enhancing dimer formation. Similarly, a more compact Gly-in compared with Gly-out homodimer would relatively stabilize the Gly-in substate.

Using a reference frame fixed to a rigid protein and the spatially dependent pressure field from a POPC environment surrounding the protein, we determined the pV work contribution to the $C99_{23-55}$ monomer and homodimer conformational equilibrium. We used a reference system consisting of a single component bilayer with pressure profile, $p(z)$. For the all-atom simulations in a POPC membrane, we estimated the impact of the pV work contributions to the conformational equilibria associated with variations in the protein volume between $C99_{23-55}$ monomer and dimers in Gly-in and Gly-out conformations (Fig. S3). The integrated pV work contribution to the formation of homodimers from separated monomer is estimated to be +0.26 kJ/mol (Gly-out) and −2.39 kJ/mol (Gly-in). This suggests that the pV work contribution to the free energy of dimerization differs between Gly-in and Gly-out by 2.65 kJ/mol favoring the formation of the Gly-in substate over the less compact Gly-out state.

Overall, we observe structures consistent with both the Gly-in and Gly-out states, with an overall ensemble that is dominated by right-handed coiled-coil structures. Moreover, the same states

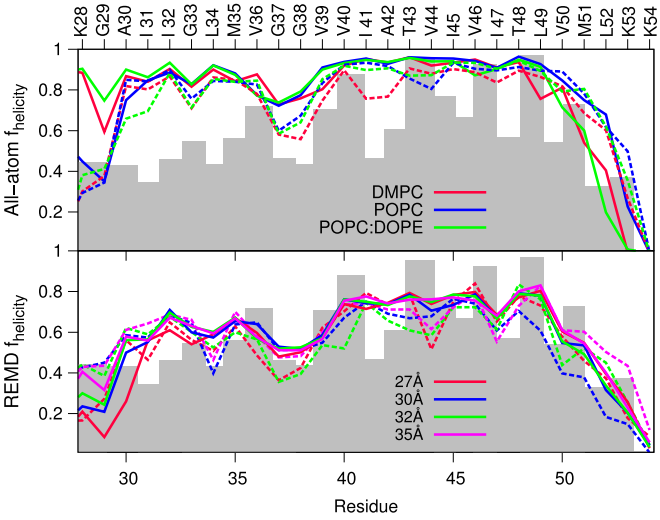

Fig. 6. Comparison of helicity derived from (*i*) all-atom simulations of $C99_{23-55}$ monomers (solid lines) and homodimer (dashed lines) in varying membrane compositions (DMPC, POPC, and POPC:DOPE in red, blue, and green, respectively) and (*ii*) all-atom REMD simulations of $C99_{23-55}$ monomers (solid lines) and homodimers (dashed lines) in implicit GBSW membrane using different membrane widths (27, 30, 32, and 35 Å in red, blue, green, and magenta). The gray shadow shows experimentally determined helicity based on NMR chemical shift measurements for monomeric $C99_{1-55}$ in an LMPG micelle (29).

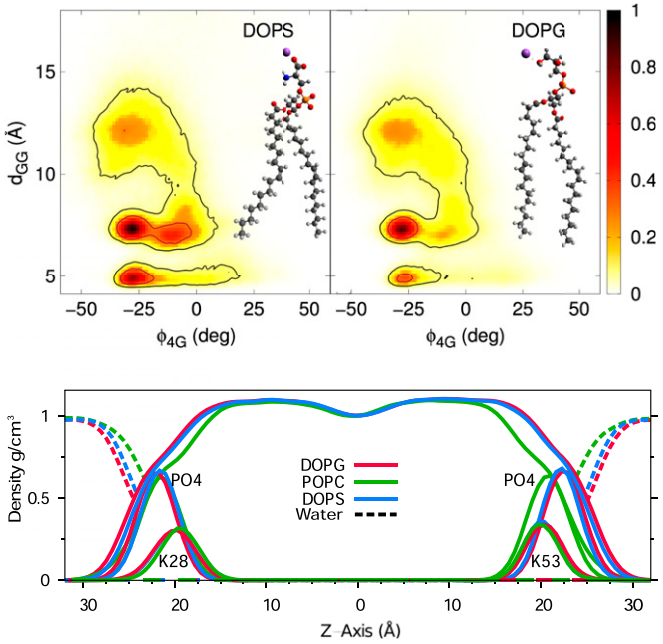

Fig. 7. The conformational distributions of ϕ_{4G} and d_{GG} in the $C99_{23-55}$ homodimers derived from CG simulations in DOPS and DOPG with their corresponding lipid structures (*Top*). Lipid, water, and phosphate group profiles are shown along with K28 and K53 density profiles of $C99_{23-55}$ homodimers in DOPG, POPC, and DOPS bilayers.

forming this structural ensemble are observed in four different membrane environments. These results based on a multiscale modeling approach that accounts for a detailed picture of the protein–lipid interactions provides clear support for the dominance of the right-handed coiled-coil structure for the WT $C99_{23-55}$ homodimer in a lipid bilayer. The simulations further suggest that lipid composition may be critical in determining the degree of helicity in the TM region, which appears to be enhanced in the homodimer relative to the monomeric peptide.

Anionic Lipids Form Thinner Bilayers in Anchoring $C99_{23-55}$ Peptides. We simulated the CG self-association of $C99_{23-55}$ dimers in single-component anionic bilayers formed by 1,2-dioleoyl-*sn*-glycero-3-phosphoserine (DOPS) or POPG lipids. We found the peptide conformational distributions in the negatively charged lipid bilayers to be strikingly similar to distributions observed in thinner PC lipid bilayers. Comparison of density profiles, for anionic (Fig. 7) and PC (Fig. 5) lipid bilayers, shows the lipid density profile is wider in the negatively charged DOPG and DOPS membranes compared with the zwitterionic POPC membrane. Despite the differences in bilayer thickness, the positions of anchoring residues K28 and K53 are nearly identical. As a consequence, the structural ensemble of the $C99_{23-55}$ dimer association in a negatively charged bilayer is comparable to that of thinner PC membrane.

Despite the similarity in the spatial distribution of anchoring residues, the overall homodimer structural ensemble is observed to be substantially broader in bilayers formed by anionic lipids. In particular, in anionic lipid bilayers there is a higher probability of Gly-out structures as well as Gly-side structures with ϕ_{4G} values near zero (Fig. 7, *Top*).

Comparison with Structural Ensembles of GpA and EphA2 Homodimers Shows Dramatic Sequence Effects. It is instructive to compare our predicted structures for $C99_{23-55}$ dimers with other well-studied membrane-spanning proteins. Among such TM proteins, dimerization of GpA is also thought to be a consequence of interactions facilitated by GxxxG motif repeats forming right-handed coiled-coils (1, 6, 35). Typically, a diversity of structures of coiled-coils interactions are found in TM helices, including homodimers or heterodimers with right- or left-handed crossing angle between the helices. Moreover, dynamic conformations of TM helix dimers are deemed to be essential for physiological function of TM proteins (36–38). One important coiled-coil TM helix is the human EphA2 receptor tyrosine kinase, which forms dimer conformations affected by the thicknesses of the lipid bilayer. In thick bilayers, EphA2 TM forms a left-handed (+15) TM dimer stabilized by a heptad repeat motif, whereas in thinner membranes the EphA2 TM dimer is characterized by a gycine zipper motif and a right-handed (−45) crossing angle between the helices (39).

The predominance of Gly-out in DOPS bilayers results from the presence in EphA2 of a GxxxG motif in the midsection of the TM helix, in contrast to the location of the GxxxG repeats in the N-terminal region of the TM helix of C99. The different location of the stabilizing motif is responsible for an enhanced Gly-out population in EphA2 relative to C99, which is particularly evident in the wide bilayers. In contrast, in thin DMPC bilayers, the Gly-in state is relatively more favorable in stabilizing EphA2 homodimers. This behavior contrasts with the relative population of Gly-in and Gly-out states in C99, which are unaffected by bilayer thickness. It is important to note that EphA2 has a GxxxG motif as well as a AxxxG motif, the latter stabilizing coiled-coiled states even when the environment disfavors direct interactions between the GxxxG interfaces (Fig. 8).

Discussion

Our multiscale simulation study, which can be readily adopted to study other membrane proteins, has demonstrated that lipid composition of membranes influences the structure and stability of $C99_{23-55}$ homodimers as well as the integrity of the TM helical region in the monomeric peptide. The monomer structure of the $C99_{23-55}$ peptides in different membrane composition is slightly modified by the membrane. The kink angle formed between the N- and C-terminal fragments of the TM helix increases with decreasing width of the hydrophobic core of the membrane. A similar effect was observed on the TM "tilt" angle, which decreases with increasing width of the membrane's hydrophobic core. At the same time, the helix stability decreases, particularly in the kink or GG hinge region, when the membrane width is diminished.

Homodimer Structures Are Conformationally Heterogeneous. The ground-state structure of the $C99_{23-55}$ dimer supports earlier predictions, based on simplified models or limited experimental

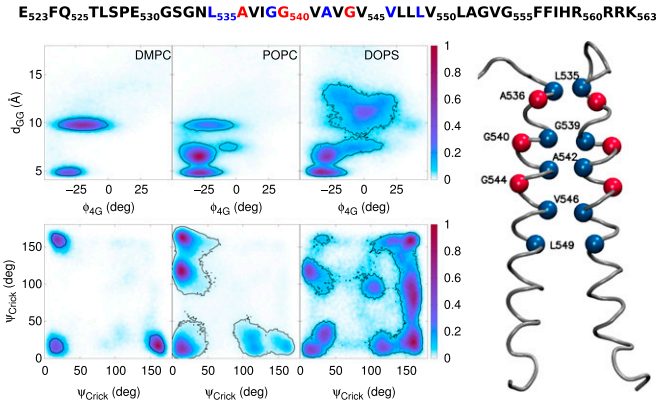

Fig. 8. EphA2 sequence (*Top*) in which residues that stabilize the Gly-out conformation preferred for wider bilayers are in blue and residues that stabilize the Gly-in conformation preferred for thinner bilayers are in red. The distributions of ϕ_{4G} and d_{GG} in the EphA2 homodimers derived from CG simulations in DMPC, POPC, and DOPS bilayer, alongside corresponding distributions of ψ_{Crick} angles. The colored scale on the *Right* defines the relative populations (*Middle* and *Bottom*). Structure of the TM fragment of EphA2 receptor (*Right* and *Bottom*) showing in blue the residues that stabilize the Gly-out conformation and in red the residues that stabilize the Gly-in conformation.

data, that the homodimer structure of $C99_{23-55}$ is a right-handed λ-like coiled-coil stabilized by interpeptide interactions. Importantly, we also find that the specific lipid composition of the membrane impacts the bilayer width, which biases the TM helix tilt orientation of the monomeric $C99_{23-55}$ structure in the membrane. The conformational ensemble is heterogeneous with the energy landscape comprising three conformational states that define the overall right-handed coiled-coil homodimer ensemble. Furthermore, the particular importance of one state relative to another is modulated by the lipid composition of the membrane bilayer. It has been previously proposed that diminished stability of the Gly-in homodimer inhibits the production of the most toxic Aβ42 isoform (40). We propose that the APP dimer structure diversity could represent an important step in APP processing and play a regulatory role in Aβ isoform distribution (24, 41). Independent of the role of homodimers in the cleavage of APP by γ-secretase, our study demonstrates quantitatively that structures of dimers are heterogeneous and that their relative population is modulated by membrane composition as well as sequence. A plausible implication of this discovery is that, even if the dimer is protected against cleavage, the shift in dimer–monomer equilibrium, achievable by variations in membrane composition, would affect Aβ product formation.

Similarity of Structures in Micelles and Thin Bilayers. The trends observed in the structural ensemble of the $C99_{23-55}$ homodimer as a function of lipid membrane composition also provide a partial explanation for the recently observed NMR structure of the $C99_{23-55}$ homodimer in DPC micelle (23, 42). The structure of $C99_{15-55}$ was observed to have a Gly-out topology that differed from the previously proposed Gly-in structures that were based on simulation and solid-state NMR data (7, 8, 43–45). The surfactant forming the DPC micelle is most similar in structure and alkyl chain length to the DMPC lipid, which has the thinnest of the four lipid bilayers studied. In DMPC bilayer, the average tilt angle was increased and the population of the Gly-out structure significantly enhanced over the structural ensembles observed in the thicker bilayers.

Multiple Factors Affect Homodimer Formation. We have identified a number of other driving forces for the formation of $C99_{23-55}$ homodimers. (1) Peptide TM helical tilt angle increases with decreasing bilayer thickness. This provides a relative stabilization of Gly-out structures in thinner membranes and micelles, and more parallel Gly-in structures in thicker bilayers. (2) The lateral pressure profile across the membrane (Fig. S3), along with varying peptide volumes between monomers and dimer (Fig. S4), as well as between competing homodimer structures, stabilizes Gly-in homodimer structures relative to separated monomers in a POPC bilayer while destabilizing Gly-out homodimers. (3) Gly-out homodimers present more hydrophilic surface area than Gly-in structures, providing a relative stabilization of Gly-out homodimers in thin bilayers and micelles in which deeper water penetration leads to greater peptide–solvent contact.

Membrane thickness impacts the processing of APP by γ-secretase and affects the overall production of Aβ peptide and the ratio of $Aβ_{40}$:$Aβ_{42}$. Our results demonstrate that membrane composition does influence membrane thickness, which can alter both the depth of insertion of the peptide into the membrane, and impact the termination of processive cleavage of the TM helix by γ-secretase. Moreover, our results show that membrane lipid composition influences the structure and stability of the C99 homodimer, with thicker membranes stabilizing Gly-in conformations. This is yet another factor that determines the processing mechanisms of C99 by γ-secretase.

Materials and Methods

We used a multiscale computational approach, combining MD and REMD simulations (46), to determine the structure of APP homodimers whose cleavage is crucial for the initiation of AD. Three distinct models were simulated (Table S1): (*i*) all-atom representations of the protein in an implicit membrane (47); (*ii*) CG models of the protein, lipids, and solvent using the Martini force field (48–50); and (*iii*) all-atom CHARMM36 force field model for the protein, membrane, and solvent environments (51–55).

Simulation details are given in *Supporting Information*.

ACKNOWLEDGMENTS. We are thankful for the resources of the Center for Computational Science at Boston University. We acknowledge the support of National Science Foundation Grants CHE-0910433 and CHE-1362524, and NIH Grant R01 GM107703. J.E.S. and L.D. thank the Schlumberger Foundation "Faculty for the Future Program" and Consejo Nacional de Ciencia y Technología for the generous support of our research.

1. Lemmon MA, et al. (1992) Glycophorin A dimerization is driven by specific interactions between transmembrane alpha-helices. *J Biol Chem* 267(11):7683–7689.
2. Senes A, Gerstein M, Engelman DM (2000) Statistical analysis of amino acid patterns in transmembrane helices: The GxxxG motif occurs frequently and in association with beta-branched residues at neighboring positions. *J Mol Biol* 296(3):921–936.
3. Arkin IT, et al. (1994) Structural organization of the pentameric transmembrane alpha-helices of phospholamban, a cardiac ion channel. *EMBO J* 13(20):4757–4764.
4. Pinto LH, et al. (1997) A functionally defined model for the M2 proton channel of influenza A virus suggests a mechanism for its ion selectivity. *Proc Natl Acad Sci USA* 94(21):11301–11306.
5. Russ WP, Engelman DM (2000) The GxxxG motif: A framework for transmembrane helix-helix association. *J Mol Biol* 296(3):911–919.
6. Senes A, Engel DE, DeGrado WF (2004) Folding of helical membrane proteins: The role of polar, GxxxG-like and proline motifs. *Curr Opin Struct Biol* 14(4):465–479.
7. Sato T, et al. (2009) A helix-to-coil transition at the ε-cut site in the transmembrane dimer of the amyloid precursor protein is required for proteolysis. *Proc Natl Acad Sci USA* 106(5):1421–1426.
8. Miyashita N, Straub JE, Thirumalai D, Sugita Y (2009) Transmembrane structures of amyloid precursor protein dimer predicted by replica-exchange molecular dynamics simulations. *J Am Chem Soc* 131(10):3438–3439.
9. Jung JI, et al. (2014) Complex relationships between substrate sequence and sensitivity to alterations in γ-secretase processivity induced by γ-secretase modulators. *Biochemistry* 53(12):1947–1957.
10. Ousson S, et al. (2013) Substrate determinants in the C99 juxtamembrane domains differentially affect γ-secretase cleavage specificity and modulator pharmacology. *J Neurochem* 125(4):610–619.
11. Ren Z, Schenk D, Basi GS, Shapiro IP (2007) Amyloid β-protein precursor juxtamembrane domain regulates specificity of γ-secretase-dependent cleavages. *J Biol Chem* 282(48):35350–35360.
12. Lichtenthaler SF, Ida N, Multhaup G, Masters CL, Beyreuther K (1997) Mutations in the transmembrane domain of APP altering γ-secretase specificity. *Biochemistry* 36(49):15396–15403.
13. Murphy MP, et al. (1999) γ-Secretase, evidence for multiple proteolytic activities and influence of membrane positioning of substrate on generation of amyloid β peptides of varying length. *J Biol Chem* 274(17):11914–11923.
14. Ehehalt R, Keller P, Haass C, Thiele C, Simons K (2003) Amyloidogenic processing of the Alzheimer β-amyloid precursor protein depends on lipid rafts. *J Cell Biol* 160(1):113–123.
15. Winkler E, et al. (2012) Generation of Alzheimer disease-associated amyloid β42/43 peptide by γ-secretase can be inhibited directly by modulation of membrane thickness. *J Biol Chem* 287(25):21326–21334.
16. Winkler E, Julius A, Steiner H, Langosch D (2015) Homodimerization protects the amyloid precursor protein c99 fragment from cleavage by γ-secretase. *Biochemistry* 54(40):6149–6152.
17. Song Y, Hustedt EJ, Brandon S, Sanders CR (2013) Competition between homodimerization and cholesterol binding to the C99 domain of the amyloid precursor protein. *Biochemistry* 52(30):5051–5064.
18. Decock M, et al. (2015) Analysis by a highly sensitive split luciferase assay of the regions involved in APP dimerization and its impact on processing. *FEBS Open Bio* 5(1):763–773.
19. Miyashita N, Straub JE, Thirumalai D (2009) Structures of β-amyloid peptide 1-40, 1-42, and 1-55—the 672-726 fragment of APP—in a membrane environment with implications for interactions with γ-secretase. *J Am Chem Soc* 131(49):17843–17852.
20. Pester O, et al. (2013) The backbone dynamics of the amyloid precursor protein transmembrane helix provides a rationale for the sequential cleavage mechanism of γ-secretase. *J Am Chem Soc* 135(4):1317–1329.
21. Lemmin T, Dimitrov M, Fraering PC, Dal Peraro M (2014) Perturbations of the straight transmembrane α-helical structure of the amyloid precursor protein affect its processing by γ-secretase. *J Biol Chem* 289(10):6763–6774.
22. Barrett PJ, et al. (2012) The amyloid precursor protein has a flexible transmembrane domain and binds cholesterol. *Science* 336(6085):1168–1171.
23. Nadezhdin KD, Bocharova OV, Bocharov EV, Arseniev AS (2012) Dimeric structure of transmembrane domain of amyloid precursor protein in micellar environment. *FEBS Lett* 586(12):1687–1692.

24. Wang H, et al. (2011) Molecular determinants and thermodynamics of the amyloid precursor protein transmembrane domain implicated in Alzheimer's disease. *J Mol Biol* 408(5):879–895.
25. Dominguez L, Meredith SC, Straub JE, Thirumalai D (2014) Transmembrane fragment structures of amyloid precursor protein depend on membrane surface curvature. *J Am Chem Soc* 136(3):854–857.
26. Dominguez L, Foster L, Meredith SC, Straub JE, Thirumalai D (2014) Structural heterogeneity in transmembrane amyloid precursor protein homodimer is a consequence of environmental selection. *J Am Chem Soc* 136(27):9619–9626.
27. Lu JX, Yau WM, Tycko R (2011) Evidence from solid-state NMR for nonhelical conformations in the transmembrane domain of the amyloid precursor protein. *Biophys J* 100(3):711–719.
28. Song Y, Mittendorf KF, Lu Z, Sanders CR (2014) Impact of bilayer lipid composition on the structure and topology of the transmembrane amyloid precursor C99 protein. *J Am Chem Soc* 136(11):4093–4096.
29. Beel AJ, et al. (2008) Structural studies of the transmembrane C-terminal domain of the amyloid precursor protein (APP): Does APP function as a cholesterol sensor? *Biochemistry* 47(36):9428–9446.
30. Cantor RS (1997) The lateral pressure profile in membranes: A physical mechanism of general anesthesia. *Biochemistry* 36(9):2339–2344.
31. Cantor RS (1999) Lipid composition and the lateral pressure profile in bilayers. *Biophys J* 76(5):2625–2639.
32. Cantor RS (1999) The influence of membrane lateral pressures on simple geometric models of protein conformational equilibria. *Chem Phys Lipids* 101(1):45–56.
33. Cantor RS (1997) Lateral pressures in cell membranes: A mechanism for modulation of protein function. *J Phys Chem B* 101(10):1723–1725.
34. Cantor RS (2002) Size distribution of barrel-stave aggregates of membrane peptides: Influence of the bilayer lateral pressure profile. *Biophys J* 82(5):2520–2525.
35. Psachoulia E, Fowler PW, Bond PJ, Sansom MS (2008) Helix-helix interactions in membrane proteins: Coarse-grained simulations of glycophorin a helix dimerization. *Biochemistry* 47(40):10503–10512.
36. Langosch D, Heringa J (1998) Interaction of transmembrane helices by a knobs-into-holes packing characteristic of soluble coiled coils. *Proteins* 31(2):150–159.
37. Javadpour MM, Eilers M, Groesbeek M, Smith SO (1999) Helix packing in polytopic membrane proteins: Role of glycine in transmembrane helix association. *Biophys J* 77(3):1609–1618.
38. Burkhard P, Stetefeld J, Strelkov SV (2001) Coiled coils: A highly versatile protein folding motif. *Trends Cell Biol* 11(2):82–88.
39. Bocharov EV, et al. (2010) Left-handed dimer of EphA2 transmembrane domain: Helix packing diversity among receptor tyrosine kinases. *Biophys J* 98(5):881–889.
40. Kienlen-Campard P, Miolet S, Tasiaux B, Octave JN (2002) Intracellular amyloid-β 1-42, but not extracellular soluble amyloid-β peptides, induces neuronal apoptosis. *J Biol Chem* 277(18):15666–15670.
41. Khalifa NB, et al. (2010) What is the role of amyloid precursor protein dimerization? *Cell Adhes Migr* 4(2):268–272.
42. Chen W, et al. (2014) Familial Alzheimers mutations within apptm increase a β42 production by enhancing accessibility of ε-cleavage site. *Nat Commun* 5:3037.
43. Munter LM, et al. (2007) GxxxG motifs within the amyloid precursor protein transmembrane sequence are critical for the etiology of Abeta42. *EMBO J* 26(6):1702–1712.
44. Scheuermann S, et al. (2001) Homodimerization of amyloid precursor protein and its implication in the amyloidogenic pathway of Alzheimer's disease. *J Biol Chem* 276(36):33923–33929.
45. Tang TC, et al. (2014) Conformational changes induced by the A21G Flemish mutation in the amyloid precursor protein lead to increased Aβ production. *Structure* 22(3):387–396.
46. Sugita Y, Okamoto Y (1999) Replica-exchange molecular dynamics method for protein folding. *Chem Phys Lett* 314(1):141–151.
47. Im W, Lee MS, Brooks CL, 3rd (2003) Generalized born model with a simple smoothing function. *J Comput Chem* 24(14):1691–1702.
48. Marrink SJ, Risselada HJ, Yefimov S, Tieleman DP, de Vries AH (2007) The MARTINI force field: Coarse grained model for biomolecular simulations. *J Phys Chem B* 111(27):7812–7824.
49. Monticelli L, et al. (2008) The martini coarse-grained force field: Extension to proteins. *J Chem Theory Comput* 4(5):819–834.
50. Stansfeld PJ, Sansom MS (2011) From coarse grained to atomistic: A serial multiscale approach to membrane protein simulations. *J Chem Theory Comput* 7(4):1157–1166.
51. Ayton GS, Voth GA (2009) Systematic multiscale simulation of membrane protein systems. *Curr Opin Struct Biol* 19(2):138–144.
52. Lyubartsev AP, Rabinovich AL (2011) Recent development in computer simulations of lipid bilayers. *Soft Matter* 7(1):25–39.
53. Marrink SJ, de Vries AH, Tieleman DP (2009) Lipids on the move: Simulations of membrane pores, domains, stalks and curves. *Biochim Biophys Acta* 1788(1):149–168.
54. Scott HL (2002) Modeling the lipid component of membranes. *Curr Opin Struct Biol* 12(4):495–502.
55. MacKerell AD, et al. (1998) All-atom empirical potential for molecular modeling and dynamics studies of proteins. *J Phys Chem B* 102(18):3586–3616.
56. Wu EL, et al. (2014) CHARMM-GUI Membrane Builder toward realistic biological membrane simulations. *J Comput Chem* 35(27):1997–2004.
57. Jo S, Kim T, Iyer VG, Im W (2008) CHARMM-GUI: A web-based graphical user interface for CHARMM. *J Comput Chem* 29(11):1859–1865.
58. Berendsen HJ, Postma JPM, van Gunsteren WF, DiNola A, Haak J (1984) Molecular dynamics with coupling to an external bath. *J Chem Phys* 81(8):3684–3690.
59. Rotkiewicz P, Skolnick J (2008) Fast procedure for reconstruction of full-atom protein models from reduced representations. *J Comput Chem* 29(9):1460–1465.
60. Jo S, Kim T, Im W (2007) Automated builder and database of protein/membrane complexes for molecular dynamics simulations. *PLoS One* 2(9):e880.